

See discussions, stats, and author profiles for this publication at: <https://www.researchgate.net/publication/5246708>

Pentanuclear and Heptanuclear Helicates By Self-Assembly of d 10 Metal Ions and a Rigid Aromatic Bis-Bidentate Chelator

ARTICLE *in* INORGANIC CHEMISTRY · AUGUST 2008

Impact Factor: 4.76 · DOI: 10.1021/ic8007969 · Source: PubMed

CITATIONS

27

READS

37

4 AUTHORS, INCLUDING:



Ai-Xin Zhu

Yunnan Normal University

20 PUBLICATIONS 378 CITATIONS

SEE PROFILE



Xiao-Ming Chen

Sun Yat-Sen University

419 PUBLICATIONS 22,293 CITATIONS

SEE PROFILE

Pentanuclear and Heptanuclear Helicates By Self-Assembly of d^{10} Metal Ions and a Rigid Aromatic Bis-Bidentate Chelator

Ai-Xin Zhu, Jie-Peng Zhang,* Yan-Yong Lin, and Xiao-Ming Chen*

MOE Laboratory of Bioinorganic and Synthetic Chemistry/State Key Laboratory of Optoelectronic Materials and Technologies, School of Chemistry & Chemical Engineering, Sun Yat-Sen University, Guangzhou 510275, China

Received May 1, 2008

The self-assembly of Zn(II) and Cd(II) ions with a bis-bidentate ligand 3,5-bis(benzimidazol-2-yl)pyrazole (H_3L) was studied by Electrospray ionization mass spectrometry, 1H NMR measurements, and single-crystal X-ray diffraction analyses. Reaction of $Zn(ClO_4)_2 \cdot 6H_2O$ and $Cd(ClO_4)_2 \cdot 6H_2O$ with H_3L in DMF gave two pentanuclear complexes $[(Zn_5(\mu_3-O)(H_2L)_6)(ClO_4)_2 \cdot DMF \cdot 9.5H_2O]$ (**1**) and $[Cd_5(\mu_3-O)(H_2L)_6](ClO_4)(OH) \cdot 4.75DMF \cdot 0.25EtOH \cdot 10.5H_2O$ (**2**), in which the trigonal-bipyramidal core structures are bridged by μ_3 -oxo and pyrazolate rings of the monodeprotonated H_2L . When $Na_3PO_4 \cdot 12H_2O$ was used in the reaction system of $CdBr_2 \cdot 4H_2O$ and H_3L , $[Cd_5(\mu_3-O)(H_2L)_6]Br_2 \cdot 4.5DMF \cdot 6.5H_2O$ (**3**) and $[Cd_7(\mu_6-PO_4)(\mu-Br)_3(H_2L)_6](HPO_4) \cdot DMF \cdot 10H_2O$ (**4**) were isolated. **3** displays the same core structure as that of **2**, whereas **4** exhibits a turbine, heptanuclear core which is bridged by a μ_6 - PO_4 , three μ -Br, and three pyrazolate rings. All of the pentanuclear and heptanuclear cores are surrounded by three pairs of bis-bidentate H_2L^- ligands with offset π – π stacking, showing propeller-like molecular structures and triple-stand helicates. Electrospray ionization mass spectrometry studies and 1H NMR measurements demonstrate that the pentanuclear complexes have different stability in the solution, depending on the metal ions and the counteranions. Furthermore, both **1** and **2** emit blue fluorescence with nanosecond luminescent lifetimes in DMF at room temperature.

Introduction

The design, synthesis, and characterization of discrete metallosupramolecular architectures have attracted great interest because of their intrinsic aesthetic appeal¹ and potential applications in catalysis,² cavity-directed synthesis,³ magnetism,⁴ and luminescent materials.⁵ Multidentate *N*-heterocyclic aromatic ligands, especially 2-fold symmetric aromatic polytopic ligands with central bridging pyridazine,

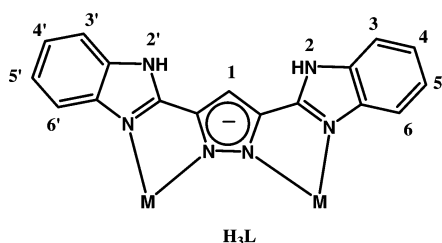
pyrimidine, tetrazine, pyrazolate, and open-chain diazine (N–N) cores have been extensively used to construct fascinating discrete metallosupramolecular structures. For example, Dunbar and co-workers have extensively studied the *N*-heterocyclic ligands 3,6-bis(2-pyridyl)-1,2,4,5-tetrazine (bptz) and 3,6-bis(2-pyridyl)pyridazine (bppn), which produced a series of structures such as dimer (M_2L_2), propeller-

* To whom correspondence should be addressed. E-mail: cxm@mail.sysu.edu.cn. Fax: Int. code +86 20 8411-2245.

- (1) (a) Stang, P. J.; Olenyuk, B. *Acc. Chem. Res.* **1997**, *30*, 502. (b) Caulder, D. L.; Raymond, K. N. *Acc. Chem. Res.* **1999**, *32*, 975. (c) Fujita, M. *Acc. Chem. Res.* **1999**, *32*, 53. (d) Holliday, B. J.; Mirkin, C. A. *Angew. Chem., Int. Ed.* **2001**, *40*, 2022. (e) Seidel, S. R.; Stang, P. J. *Acc. Chem. Res.* **2002**, *35*, 972. (f) Leininger, S.; Bogdan Olenyuk, P. J.; Stang, *Chem. Rev.* **2000**, *100*, 853. (g) Davis, A. V.; Yeh, R. M.; Raymond, K. N. *Proc. Natl. Acad. Sci. U.S.A.* **2002**, *99*, 4793. (h) Fujita, M.; Tominaga, M.; Hori, A.; Therrien, B. *Acc. Chem. Res.* **2005**, *38*, 371. (i) Kuehl, C. J.; Kryshenko, Y. K.; Radhakrishnan, U.; Seidel, S. R.; Huang, S. D.; Stang, P. J. *Proc. Natl. Acad. Sci. U.S.A.* **2002**, *99*, 4932.
- (2) (a) Merlau, M. L.; Mejia, M. d. P.; Nguyen, S. T.; Hupp, J. T. *Angew. Chem., Int. Ed.* **2001**, *40*, 4239. (b) Fiedler, D.; Leung, D. H.; Bergman, R. G.; Raymond, K. N. *Acc. Chem. Res.* **2005**, *38*, 351.

- (3) (a) Lützen, A. *Angew. Chem., Int. Ed.* **2005**, *44*, 1000. (b) Vriezema, D. M.; Aragonès, M. C.; Elemans, J. A. A. W.; Cornelissen, J. J. L. M.; Rowan, A. E.; Nolte, R. J. M. *Chem. Rev.* **2005**, *105*, 1445. (c) Nishioka, Y.; Yamaguchi, T.; Yoshizawa, M.; Fujita, M. *J. Am. Chem. Soc.* **2007**, *129*, 7000.
- (4) (a) Thompson, L.; K., *Coord. Chem. Rev.* **2002**, *233–234*, 193. (b) Thompson, L. K.; Waldmann, O.; Xu, Z. *Coord. Chem. Rev.* **2005**, *249*, 2677. (c) Zheng, Y.-Z.; Xue, W.; Zhang, W.-X.; Tong, M.-L.; Chen, X.-M. *Inorg. Chem.* **2007**, *46*, 6437.
- (5) (a) Lai, S.-W.; Chan, C.-W. M.; Peng, S.-M.; Che, C.-M. *Angew. Chem., Int. Ed.* **1999**, *38*, 669. (b) Sapochak, L. S.; Benincasa, F. E.; Schofield, R. S.; Baker, J. L.; Riccio, K. K. C.; Fogarty, D.; Kohlmann, H.; Ferris, K. F.; Burrows, P. E. *J. Am. Chem. Soc.* **2002**, *124*, 6119. (c) Zheng, X.-L.; Liu, Y.; Pan, M.; Lü, X.-Q.; Zhang, J.-Y.; Zhao, C.-Y.; Tong, Y.-X.; Su, C.-Y. *Angew. Chem., Int. Ed.* **2007**, *46*, 7399. (d) Tong, Y.-P.; Zheng, S.-L.; Chen, X.-M. *Inorg. Chem.* **2005**, *44*, 4270. (e) Zhang, J.-P.; Lin, Y.-Y.; Huang, X.-C.; Chen, X.-M. *Eur. J. Inorg. Chem.* **2006**, *17*, 3407.

Chart 1



type (M_2L_3), 2×2 grid-type (M_4L_4), and pentagon-type (M_5L_5) species.⁶ Constable et al. reported the self-assembly of silver(I) with a 4-substituent bppn ligand, which yielded a centered-tetrahedral (Ag_5L_4) species.⁷ Thompson et al. demonstrated the powerful ability of aromatic polytopic diazine ligands with open-chain diazine (N–N) cores for the self-assembly of a series of structures such as tetranuclear square grids (M_4L_4), trigonal-bipyramidal clusters (M_5L_6), $[3 \times 3]$ grids (M_9L_6), hexadecanuclear $4 \times [2 \times 2]$ M^{II}_{16} square grids, Cu_8 pinwheels, and a spheroidal Cu_{36} cluster.⁸ Although various species have been constructed by aromatic bis-bidentate ligands, very few examples of polynuclear helicates have been reported.⁹

Previously, we have shown that copper(I) 3,5-bis(pyridin-2-yl)triazolate can self-assemble to yield a 2×2 grid-type complex and three 1D supramolecular isomers.¹⁰ As a consequence, we extended our study to another rigid, bis-bidentate *N*-heterocyclic ligand, 3,5-bis(benzimidazol-2-yl)pyrazole (H_3L , Chart 1), which may have similar coordination mode as *syn*-3,5-bis(pyridin-2-yl)triazole and 3,5-bis(pyridin-2-yl)pyrazolate (Hpypz). Extensive studies have shown that such ligands with central bridging five-

membered heterocycles tend to form mononuclear,¹¹ binuclear,¹² and 2×2 grid-type structures.¹³ Very recently, several pentanuclear triple-helical complexes, such as $[Fe_5(\mu_3-O)(pypz)_6]^{2+}$ and $[M_5(\mu_3-OH)(pypz)_6]^{3+}$ ($M = Ni^{2+}$ or Zn^{2+}) have been characterized in the solid state.⁹ Nevertheless, the stabilities of these complexes in the solution have not been studied. Herein, we report our systematic studies of the self-assembly of d^{10} metal ions [$Zn(II)$ and $Cd(II)$] with H_3L . Two novel helicates with pentanuclear trigonal-bipyramidal cores $[M_5(\mu_3-O)(H_2L)_6]^{2+}$ and a turbinat, heptanuclear helicate $[Cd_7(\mu_6-PO_4)(\mu-Br)_3(H_2L)_6]^{2+}$ have been verified by means of electrospray ionization mass spectrometry, 1H NMR, and/or single-crystal X-ray diffraction analyses.

Experimental Section

Materials and Physical Measurements. Commercially available reagents were used as received without further purification. The ligand H_3L was prepared according to the procedure reported in the literature.¹⁴ IR spectra were obtained from KBr pellets on a Bruker EQUINOX 55 FTIR spectrometer in the 400–4000 cm^{-1} region. Elemental analyses (C, H, N) were performed with a Vario EL elemental analyzer. ESI-MS spectra were performed on a Thermo Finnigan LCQ DECA XP quadrupole ion trap mass spectrometer using an electrospray ionization source with MeCN as the mobile phase. All spectra were acquired in the positive ion mode, and the spray voltage was set at 4500 V. 1H and $\{^1H-^1H\}$ COSY NMR spectra were recorded on a Varian Mercury-Plus 300 NMR spectrometer using DMSO- d_6 solution at 298 K, and the chemical shifts were referenced to the residual proton impurities of the deuterated solvent (DMSO- d_6). UV–vis spectra were performed on a Varian Cary 300 UV–vis Spectrophotometer at room temperature. The steady-state fluorescent spectra were measured on a SHIMADZU RF-5301PC spectrofluorophotometer. Lifetime measurements were performed on an Edinburgh FLS920 spectrometer equipped with an nF900 ns flash lamp. Lifetime data were fitted with single- or double-exponential decay functions.

Preparation of the Complexes. **CAUTION.** Perchlorate salts are potentially explosive and therefore should be handled with care!

$[(Zn_5(\mu_3-O)(H_2L)_6)(ClO_4)_2 \cdot DMF \cdot 9.5H_2O]$ (**1**). To a solution of $Zn(ClO_4)_2 \cdot 6H_2O$ (37 mg, 0.1 mmol) in ethanol (4 mL) was added

- (6) (a) Campos-Fernández, C. S.; Clérac, R.; Dunbar, K. R. *Angew. Chem., Int. Ed.* **1999**, *38*, 3477. (b) Campos-Fernández, C. S.; Schottel, B. L.; Chifotides, H. T.; Bera, J. K.; Bacsá, J.; Koomen, J. M.; Russell, D. H.; Dunbar, K. R. *J. Am. Chem. Soc.* **2005**, *127*, 12909. (c) Schottel, B. L.; Bacsá, J.; Dunbar, K. R. *Chem. Commun.* **2005**, 46. (d) Schottel, B. L.; Chifotides, H. T.; Shatruck, M.; Chouai, A.; Pérez, L. M.; Bacsá, J.; Dunbar, K. R. *J. Am. Chem. Soc.* **2006**, *128*, 5895.
- (7) Constable, E. C.; Housecroft, C. E.; Neuburger, M.; Reymann, S.; Schaffner, S. *Chem. Commun.* **2004**, 1056.
- (8) (a) Matthews, C. J.; Xu, Z.; Mandal, S. K.; Thompson, L. K.; Biradha, K.; Poirier, K.; Zaworotko, M. J. *Chem. Commun.* **1999**, 347. (b) Matthews, C. J.; Thompson, L. K.; Parsons, S. R.; Xu, Z.; Miller, D. O.; Heath, S. L. *Inorg. Chem.* **2001**, *40*, 4448. (c) Dawe, L. N.; Abedin, T. S. M.; Kelly, T. L.; Thompson, L. K.; Miller, D. O.; Zhao, L.; Wilson, C.; Leechb, M. A.; Howardb, J. A. K. *J. Mater. Chem.* **2006**, *16*, 2645. (d) Dey, S. K.; Thompson, L. K.; Dawe, L. N. *Chem. Commun.* **2006**, 4967. (e) Thompson, L. K.; Kelly, T. L.; Dawe, L. N.; Grove, H.; Lemaire, M. T. *Inorg. Chem.* **2004**, *43*, 7605. (f) Dawe, L. N.; Thompson, L. K. *Angew. Chem., Int. Ed.* **2007**, *46*, 7440. (g) Milway, V. A.; Niel, V.; Abedin, T. S. M.; Xu, Z.; Thompson, L. K.; Grove, H.; Miller, D. O.; Parsons, S. R. *Inorg. Chem.* **2004**, *43*, 1874. (h) Abedin, T. S. M.; Thompson, L. K.; Miller, D. O.; Krupicka, E. *Chem. Commun.* **2003**, 708. (i) Niel, V.; Milway, V. A.; Dawe, L. N.; Grove, H.; Tandon, S. S.; Abedin, T. S. M.; Kelly, T. L.; Spencer, E. C.; Howard, J. A. K.; Collins, J. L.; Miller, D. O.; Thompson, L. K. *Inorg. Chem.* **2008**, *47*, 176.
- (9) (a) Yoneda, K.; Adachi, K.; Nishio, K.; Yamasaki, M.; Fuyuhro, A.; Katada, M.; Kaizaki, S.; Kawata, S. *Angew. Chem., Int. Ed.* **2006**, *45*, 5459. (b) Hou, J.-Z.; Li, M.; Li, Z.; Zhan, S.-Z.; Huang, X.-C.; Li, D. *Angew. Chem., Int. Ed.* **2008**, *47*, 1711.
- (10) Zhang, J.-P.; Lin, Y.-Y.; Huang, X.-C.; Chen, X.-M. *Chem. Commun.* **2005**, 1258.

- (11) (a) Hartmann, U.; Vahrenkamp, H. *Inorg. Chim. Acta* **1995**, *239*, 13. (b) Jircitano, A. J.; Sommerer, S. O.; Abboud, K. A. *Acta Crystallorg., Sect. C* **1997**, *53*, 434. (c) Moliner, N.; Muñoz, M. C.; Létard, S.; Létard, J.-F.; Solans, X.; Burriel, R.; Castro, M.; Kahn, O.; Real, J. A. *Inorg. Chim. Acta* **1999**, *291*, 279. (d) Zhu, D.-R.; Song, Y.; Xu, Y.; Zhang, Y.; Raj, S. S. S.; Fun, H.-K.; You, X.-Z. *Polyhedron* **2000**, *19*, 2019. (e) Zhu, D.-R.; Xu, Y.; Yu, Z.; Guo, Z.-J.; Sang, H.; Liu, T.; You, X.-Z. *Chem. Mater.* **2002**, *14*, 838. (f) Zhang, S.-P.; Shao, S.-C.; Liu, Z.-D.; Zhu, H.-L. *Acta Crystallorg., Sect. E* **2005**, *61*, m799. (g) Klingele, M. H.; Noble, A.; Boyd, P. D.W.; Brooker, S. *Polyhedron* **2007**, *26*, 479.
- (12) (a) Casabó, J.; Pons, J.; Siddiqi, K. S.; Teixidor, F.; Molins, E.; Miravittles, C. *J. Chem. Soc., Dalton Trans.* **1989**, 1401. (b) Shao, S.-C.; You, Z.-L.; Zhang, S.-P.; Zhu, H.-L.; Ng, S. W. *Acta Crystallorg., Sect. E* **2005**, *61*, m265. (c) Yoneda, K.; Nakano, K.; Fujioka, J.; Yamada, K.; Suzuki, T.; Fuyuhro, A.; Kawata, S.; Kaizaki, S. *Polyhedron* **2005**, *24*, 2437. (d) Du, M.; Chen, S.-T.; Guo, Y.-M.; Bu, X.-H.; Ribas, J. J. *Mol. Struct.* **2005**, *737*, 15. (e) Klingele, M. H.; Boyd, P. D. W.; Moubaraki, B.; Murray, K. S.; Brooker, S. *Eur. J. Inorg. Chem.* **2005**, 910. (f) Klingele, M. H.; Boyd, P. D. W.; Moubaraki, B.; Murray, K. S.; Brooker, S. *Eur. J. Inorg. Chem.* **2006**, 573. (g) Cheng, L.; Zhang, W.-X.; Ye, B.-H.; Lin, J.-B.; Chen, X.-M. *Inorg. Chem.* **2007**, *46*, 1135.
- (13) Pons, J.; Sanchez, F. J.; Casabó, J.; Alvarez-Larena, A.; Piniella, J. F.; Ros, J. *Inorg. Chem. Commun.* **2003**, *6*, 833.
- (14) (a) Baitalik, S.; Flörke, U.; Nag, K. *J. Chem. Soc., Dalton Trans.* **1999**, 719.

Table 1. Summary of the Crystal Data and Structure Refinements for **1**, **2**, and **4**^a

compound	1	2	4
formula	C ₁₀₅ H ₉₂ Cl ₂ N ₃₇ O _{19.5} Zn ₅	C _{116.75} H _{122.75} Cd ₅ ClN _{40.75} O _{21.5}	C ₁₀₅ H ₉₄ Br ₃ Cd ₇ N ₃₇ O ₁₉ P ₂
fw	2581.95	3038.24	3266.64
cryst syst	monoclinic	triclinic	cubic
space group	<i>P</i> 2 ₁ / <i>n</i>	<i>P</i> $\bar{1}$	<i>Pa</i> $\bar{3}$
<i>a</i> (Å)	25.789(3)	21.521(3)	29.7407(6)
<i>b</i> (Å)	14.8820(15)	22.793(3)	29.7407(6)
<i>c</i> (Å)	31.250(3)	33.219(5)	29.7407(6)
α (deg)	90	100.886(13)	90
β (deg)	95.858(2)	102.474(13)	90
γ (deg)	90	106.373(12)	90
<i>V</i> (Å ³)	11 931(2)	14 713(4)	26 305.9(9)
<i>Z</i>	4	4	8
<i>D</i> _{calcd} (g cm ⁻³)	1.427	1.362	1.639
μ (mm ⁻¹)	1.115	6.468	2.119
GOF	1.038	1.014	1.022
R1 [<i>I</i> > 2 σ (<i>I</i>)]	0.0735	0.0679	0.0710
wR2 [all data]	0.2314	0.2218	0.2213

$$^a \text{R1} = \sum |F_o| - |F_c| / \sum |F_o|; \text{wR2} = [\sum w(F_o^2 - F_c^2)^2 / \sum w(F_o^2)]^{1/2}.$$

a DMF solution (8 mL) containing H₃L (30 mg, 0.1 mmol). After a solution of KOH (11 mg, 0.2 mmol) in H₂O (0.5 mL) was added, the light-yellow mixture was stirred for 30 min, filtered, and allowed to stand at room temperature. X-ray quality yellow needle-shaped crystals formed after three weeks (yield 70%). Anal. Calcd (%) for C₁₀₅H₉₂Cl₂N₃₇O_{19.5}Zn₅: C, 48.84; H, 3.59; N, 20.07. Found C, 48.68; H, 3.65; N, 19.93. ¹H NMR (300 MHz, DMSO-*d*₆, δ): 13.60 (br, 6H, 2-H), 13.08 (d, 6H, 2'-H), 7.89 (s, DMF), 7.67 (6H, d, *J* = 8.0 Hz, 3-H), 7.44 (6H, d, *J* = 8.0 Hz, 3'-H), 7.20 (6H, t, *J* = 7.6 Hz, 4-H), 6.98 (6H, t, *J* = 7.5 Hz, 4'-H), 6.70 (6H, dd, *J* = 7.0 Hz, 5-H), 6.26 (6H, d, *J* = 3.1 Hz, 1-H), 5.78 (6H, d, *J* = 8.1 Hz, 6-H), 5.71 (d, 6H, *J* = 8.2 Hz, 6'-H), 5.58 (6H, dd, *J* = 7.0 Hz, 5'-H). IR (cm⁻¹, KBr): 3405, 3106 (s, br), 1658(s), 1591(s), 1499(w), 1475(m), 1433(s), 1381(s), 1336(w), 1278(s), 1146(s), 1091(s, ν ClO₄⁻), 1050(m), 1030(m), 813(w), 746(s), 664(w), 629(m), 577(m), 542(w), 435(m).

[Cd₅(μ_3 -O)(H₂L)₆](ClO₄)(OH)·4.75DMF·0.25EtOH·10.5-H₂O (**2**). A procedure similar to that described for the synthesis of **1** was carried out with Cd(ClO₄)₂·6H₂O (42 mg, 0.1 mmol), H₃L (30 mg, 0.1 mmol), and NaOH (4 mg, 0.1 mmol). Yield: 45%. Anal. Calcd for C_{116.75}H_{122.75}Cd₅ClN_{40.75}O_{21.5}: C, 46.15; H, 4.07; N, 18.79. Found C, 50.15; H, 3.85; N, 19.05. The crystals of **2** are easy to lose some solvents in air at room temperature, giving the molecular formula as [Cd₅(μ_3 -O)(H₂L)₆](OH)(ClO₄)·4DMF·5H₂O. Anal. Calcd (%) for C₁₁₄H₁₀₅Cd₅ClN₄₀O₁₅: C, 47.66; H, 3.68; N, 19.50. Found C, 47.58; H, 3.55; N, 19.59. ¹H NMR (300 MHz, DMSO-*d*₆, δ): 13.70–13.21 (m, 12H, 2-H and 2'-H), 7.92 (4H, s, DMF), 7.75 (6H, d, *J* = 7.7 Hz, 3-H), 7.56 (6H, d, *J* = 7.6 Hz, 3'-H), 7.30 (6H, t, *J* = 7.4 Hz, 4-H), 7.12 (6H, t, *J* = 6.6 Hz, 4'-H), 6.88 (6H, t, *J* = 7.1 Hz, 5-H), 6.52 (6H, d, *J* = 7.8 Hz, 6-H), 6.30 (6H, s, 1-H), 6.08(12H, m, 5'-H and 6'-H). IR (cm⁻¹, KBr): 3410(s, br), 1657(s), 1626 (s), 1588(s), 1465(m), 1428(s), 1378(s), 1377(w), 1277(m), 1233(w), 1115(vs, ν ClO₄⁻), 1049(m), 967(w), 808(w), 745(s), 629(m), 572(w), 536(w), 432(w).

[Cd₅(μ_3 -O)(H₂L)₆Br₂·4.5DMF·6.5H₂O(**3**)and[Cd₇(μ_6 -PO₄)(μ -Br)₃(H₂L)₆](HPO₄)·DMF·10H₂O (**4**). To a DMF solution (8 mL) of H₃L (30 mg, 0.1 mmol) was added a solution of CdBr₂·4H₂O (69 mg, 0.2 mmol) in MeOH (8 mL) to give a light-yellow clear solution. The mixture stirred for 10 min, and then a solution of Na₃PO₄·12H₂O (13 mg, 0.035 mmol) in H₂O (0.5 mL) was added. The result solution was filtered and allowed to stand at room temperature for three weeks and pale-yellow block-shaped crystals of **3** (yield 48%) and yellow polyhedral crystals of **4** (yield 4%) appeared. The two compounds were manually separated, dried at the vacuum condition. Although the single-crystal structure of **3**

could not be refined properly due to poor reflection data, a preliminary structural solution gives a similar pentanuclear cluster as that of **2**. The molecular formula of **3** is assigned from elemental analysis and IR spectroscopy as [Cd₅(μ_3 -O)(H₂L)₆Br₂·4.5DMF·6.5H₂O. Anal. Calcd (%) for C_{115.5}H_{110.5}Br₂Cd₅N_{40.5}O₁₂: C, 46.56; H, 3.74; N, 19.04. Found C, 46.35; H, 3.78; N, 18.93. IR (cm⁻¹, KBr): 3340, 3192(s, br), 1658(s), 1687(s), 1496(w), 1465(m), 1427(s), 1378(s), 1336(w), 1277(s), 1231(w), 1101(w), 1047(m), 967 (w), 808 (w), 745(s), 670(w), 614(w), 572(w), 536(w), 431(w). Polyhedral crystals of **4** are suitable for X-ray diffraction. Anal. Calcd (%) for C₁₀₅H₉₄Br₃Cd₇N₃₇O₁₉P₂: C, 38.61; H, 2.90; N, 15.86. Found C, 38.76; H, 2.93; N, 15.79. IR (cm⁻¹, KBr): 3416, 3154(s, br), 1565(s), 1589(s), 1497(m), 1465(s), 1431(s), 1379(s), 1338(w), 1278(m), 1050(s, br, ν PO₄³⁻), 807(w), 744(s), 573(m), 539(w), 434(w).

X-ray Crystallography. Single-crystal X-ray data for **1** and **3** were collected at 150(2) K on a Bruker Apex CCD area-detector diffractometer equipped with a graphite-monochromated Mo K α radiation (λ = 0.71073 Å) in a cold stream of liquid nitrogen. The raw data for the two structures were processed using *SAINT* and absorption corrections were applied using *SADABS*.¹⁵ The intensity data for **2** were collected at 150(2) K on an Oxford Gemini S Ultra diffractometer with the enhanced X-ray source of copper radiation (λ = 1.54178 Å) using the ω - ϕ scan technique. Empirical absorption correction was applied using spherical harmonics implemented in the *SCALE3 ABSPACK* scaling algorithm.¹⁶ All of the structures were solved by direct methods and refined by full-matrix least-squares based on *F*² using the *SHELXTL* program package.¹⁷ Anisotropic thermal parameters were applied to all non-hydrogen atoms and some disordered atoms. The hydrogen atoms were generated geometrically (C–H 0.96 Å, N–H 0.86 Å). Crystal data as well as details of data collection and refinements for the complexes are summarized in Table 1.

Results and Discussion

Syntheses, ESI-MS Spectra, and ¹H NMR Studies. As the ligand H₃L only dissolves in DMF and DMSO, we carried out the experiments in DMF. Upon addition of KOH

(15) Sheldrick, G. M. *SADABS 2.05, Program for Empirical Absorption Correction of Area Detector Data*; University of Göttingen: Göttingen, Germany, 1996.

(16) *CrysAlis CCD and RED*, Oxford Diffraction Ltd., Version 1.171.31.7, 2006.

(17) *SHELXTL 6.10*; Bruker Analytical Instrumentation: Madison, WI, 2000.

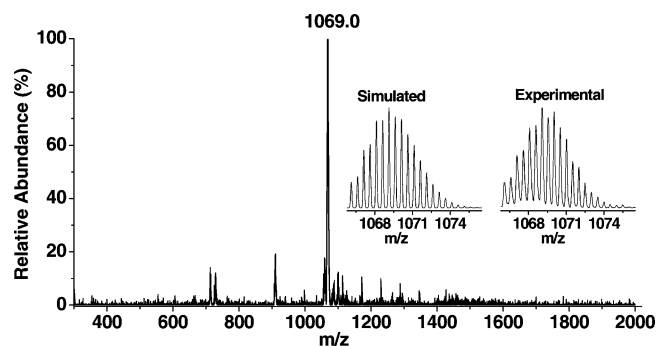


Figure 1. ESI-MS of H_3L in the presence of $\text{Zn}(\text{ClO}_4)_2 \cdot 6\text{H}_2\text{O}$ (1 equiv) and KOH (2 equiv) in DMF- H_2O (v/v 16:1) solution (the ion signals correspond to $[\text{Zn}_5(\mu_3\text{-O})(\text{H}_2\text{L})_6]^{2+}$). The experimental and theoretical isotopic distribution patterns of $[\text{Zn}_5(\mu_3\text{-O})(\text{H}_2\text{L})_6]^{2+}$ are shown in the inset.

to the DMF solution of $\text{Zn}(\text{ClO}_4)_2 \cdot 6\text{H}_2\text{O}$ and H_3L , the ESI-MS spectrum obviously shows the main ion signal at m/z 1069.0 (Figure 1). This signal does not match the common structures such as the mononuclear, binuclear, and 2×2 grid-type ones, but implies an oxo-centered pentanuclear $[\text{Zn}_5\text{O}(\text{H}_2\text{L})_6]^{2+}$ unit. The experimental and theoretical isotopic distribution patterns are identical for this pentanuclear unit. Furthermore, slow evaporation of the resulting solution yields X-ray quality crystals $[(\text{Zn}_5(\mu_3\text{-O})(\text{H}_2\text{L})_6)(\text{ClO}_4)_2 \cdot \text{DMF} \cdot 9.5\text{H}_2\text{O}]$ (**1**).

When we used $\text{Cd}(\text{ClO}_4)_2 \cdot 6\text{H}_2\text{O}$ to replace $\text{Zn}(\text{ClO}_4)_2 \cdot 6\text{H}_2\text{O}$, the ESI mass spectrum of a DMF-EtOH solution of $\text{Cd}(\text{ClO}_4)_2 \cdot 6\text{H}_2\text{O}$, H_3L , and NaOH exhibits multiple peaks of cationic species (Figure S1 in the Supporting Information), implying that the self-assembly yields multiple products. Nevertheless, the main peaks at 1186.9 can be assigned to $[\text{Cd}_5\text{O}(\text{H}_2\text{L})_6]^{2+}$, and slow evaporation of the resulting solution gave crystals of $[\text{Cd}_5(\mu_3\text{-O})(\text{H}_2\text{L})_6](\text{ClO}_4)(\text{OH}) \cdot 4.75\text{DMF} \cdot 0.25\text{EtOH} \cdot 10.5\text{H}_2\text{O}$ (**2**). When $\text{Na}_3\text{PO}_4 \cdot 12\text{H}_2\text{O}$ was added to the DMF- H_2O solution of $\text{CdBr}_2 \cdot 4\text{H}_2\text{O}$ and H_3L , the ESI-MS spectrum also exhibits a series of ion peaks (Figure S2 in the Supporting Information). Besides the pentanuclear cation, higher-nuclear structure can also be detected. Despite a very weak ion signal, the peak at m/z 1459.0 may be ascribed to $[\text{Cd}_7(\text{PO}_4)(\text{Br}_3)(\text{H}_2\text{L})_6]^{2+}$. By slow evaporation of a DMF-MeOH- H_2O solution of $\text{CdBr}_2 \cdot 4\text{H}_2\text{O}$, H_3L and $\text{Na}_3\text{PO}_4 \cdot 12\text{H}_2\text{O}$, pale-yellow block-shaped crystals of $[\text{Cd}_5(\mu_3\text{-O})(\text{H}_2\text{L})_6]\text{Br}_2 \cdot 4.5\text{DMF} \cdot 6.5\text{H}_2\text{O}$ (**3**) and yellow polyhedral crystals of $[\text{Cd}_7(\mu_6\text{-PO}_4)(\mu\text{-Br})_3(\text{H}_2\text{L})_6](\text{HPO}_4) \cdot \text{DMF} \cdot 10\text{H}_2\text{O}$ (**4**) can be isolated. Nevertheless, treatment of the DMF- H_2O solution of **3** with $\text{CdBr}_2 \cdot 4\text{H}_2\text{O}$ and $\text{Na}_3\text{PO}_4 \cdot 12\text{H}_2\text{O}$ at room temperature over several days cannot generate the heptanuclear unit as confirmed by ESI-MS technique, indicating that the pentanuclear complex cannot transform to the heptanuclear one. In other words, the heptanuclear compound is a kinetic product during the process of self-assembly.

To verify the solution structures, we also performed ^1H NMR studies for these clusters. The aromatic region of the ^1H NMR spectrum of **1** in d_6 -DMSO exhibits 11 sets of resonances (Figure 2), which indicates that the six H_2L^- ligands of **1** are equivalent and the H_2L^- ligands are bound to Zn^{2+} ions in an asymmetric fashion. In other words, there

is no C_2 axis passing through the ligand backbone. The upfield shift of the signals for most of the phenyl protons of **1** as compared to those of H_3L , which might be attributed to the shielding effect from the neighboring aromatic rings, indicating that **1** involves intramolecular π - π stacking interactions. The distinct signals at 13.60 and 13.08 ppm in the most downfield region are assigned to the two benzimidazole N-H protons (H_2 and H_2'), confirming that the imidazole groups are not deprotonated. The ^1H - ^1H COSY spectrum is particularly useful to locate the spin couplings of the aromatic protons of the benzimidazole group (Figure 3). The signals at 6.26 ppm should be assigned to H_1 because there is no hydrogen to couple with it. The assignments of other protons of the benzimidazole are facilitated by taking into consideration of the following facts.^{14,18} The usual decreased order of chemical shifts is $\text{H}_3 > \text{H}_4 > \text{H}_5 > \text{H}_6$ ($\text{H}_3' > \text{H}_4' > \text{H}_5' > \text{H}_6'$); the protons H_3 and H_6 are normally observed as doublets, whereas H_4 (H_4') and H_5 (H_5') appear either as triplet or doublet of doublet. Therefore, the resonances at 7.67, 7.20, 6.70, and 5.78 ppm are ascribed to H_3 , H_4 , H_5 , and H_6 , respectively, whereas the resonances at 7.44, 6.98, 5.71, and 5.58 ppm belong to H_3' , H_4' , H_6' , and H_5' , respectively. The H_5' and H_6' resonances are not in accordance with the aforementioned rule because the H_5' proton may experience maximum diamagnetic shielding by the anisotropic ring current of the adjacent H_2L^- ligand. This unsymmetrical shielding effect can be ascribed to an offset face-to-face stacking of H_2L^- . According to the ESI-MS and ^1H NMR spectra, we can speculate that **1** may exhibit similar structure as the reported pentanuclear propeller-shaped structure.^{9a}

For **2**, the aromatic region of the ^1H NMR spectrum in d_6 -DMSO exhibits nine sets of peaks, indicating some resonances (H_2 and H_2' , H_5' and H_6') are overlapped (Figure S3 in the Supporting Information). The assignments of the signals have also been achieved with the help of the 2D-COSY spectrum (Figure S4 in the Supporting Information). The shielding effect from the neighboring aromatic rings makes some of the phenyl protons (H_1 , H_5 , H_5' , H_6 , and H_6') shift to the upfield as compared to those of the free H_3L ligand. However, all proton signals on the phenyl and pyrazole rings of **2** are shifted downfield from those of **1** (Table S1 in the Supporting Information). These results show **2** may exhibit weaker aromatic π - π stacking interactions than that of **1**.

In contrast to **1** and **2**, **3** is very unstable in DMF and DMSO and decomposes into a white precipitate when the solution stands at the room temperature for several hours. When **3** was dissolved in d_6 -DMSO solution and we immediately performed an NMR measurement, the main signals exhibit the similar chemical shifts as **1** (Figure S5 in the Supporting Information). The ESI-MS spectrum also shows the main peaks at 1186.9 corresponding to $[\text{Cd}_5\text{O}(\text{H}_2\text{L})_6]^{2+}$ (Figure S6 in the Supporting Information). These observations indicate that **3** has a similar core structure as that in **2**.

(18) (b) Baitalik, S.; Flörke, U.; Nag, K. *Inorg. Chem.* **1999**, *38*, 3296. (c) Baitalik, S.; Bag, P.; Nag, K. *Polyhedron* **2002**, *21*, 2481. (d) Baitalik, S.; Dutta, B.; Nag, K. *Polyhedron* **2004**, *23*, 913.

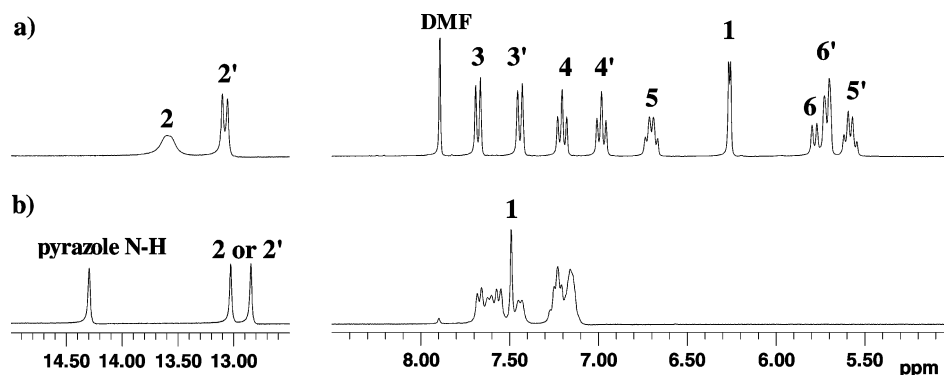


Figure 2. Aromatic region of the ^1H NMR spectrum of **1** (a) and H_3L (b) in $\text{DMSO}-d_6$ (some heavily overlapped protons of the H_3L ligand are not assigned).

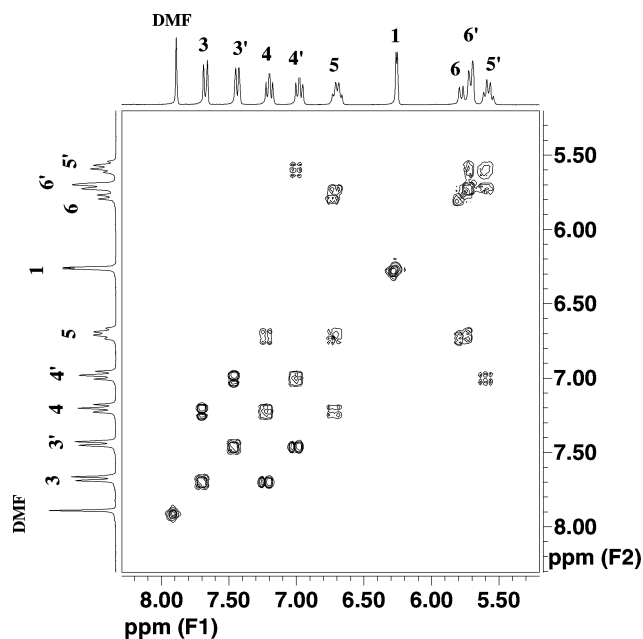


Figure 3. $\{^1\text{H}-^1\text{H}\}$ COSY NMR spectrum of **1** in $\text{DMSO}-d_6$.

As **4** is virtually insoluble in common solvents, no structural information of **4** can be elucidated from NMR analysis. Nevertheless, the good quality single crystals of **4** allowed us to determine its structure by single X-ray crystallography.

It is noteworthy that the stabilities of these pentanuclear compounds are different in solution, although they have similar core structures. **1** is very stable in DMSO because its ^1H NMR spectrum does not change for several months, whereas **2** decomposes into a white insoluble material in DMF or DMSO for about 1 week. **3** is the most unstable species in solution as it starts to decompose as soon as being dissolved. Considering the similar core structures of these compounds, their stability difference might be explained by that the smaller $\text{Zn}(\text{II})$ ion holds the cluster more compactly than the large $\text{Cd}(\text{II})$ ion. Meanwhile, the strong-coordinating bromide tends to bond to the metal and accelerate the decomposition of the cluster. Therefore, it can be concluded that the solution stabilities of these clusters are strongly affected by the metal ions and the counteranions.

X-ray Crystal Structures. The single-crystal X-ray structural analysis indicates that **1** is indeed a pentanuclear structure, in accord with the ESI-MS and NMR studies. The structure of

a $\Delta\Delta$ -configurational cation of **1** is illustrated in Figure 4a. Three pairs of bis-bidentate H_2L ligands with offset face-to-face π - π stacking are arranged around the pentanuclear, trigonal-bipyramidal zinc(II) core in a propeller-like form to generate a supramolecular *P* helix with a quasi- D_3 molecular symmetry (crystallographic C_2 symmetry). As shown in Figure 4b, the core structure of the cation contains an equilateral triangle of zinc ions ($\text{Zn}2$, $\text{Zn}3$, and $\text{Zn}3\text{A}$) with a μ_3 -oxo anion in the center. Each zinc atom in the triangular plane shows a distorted trigonal-bipyramidal geometry, being coordinated by four nitrogen atoms from two chelating H_2L^- ligands and a μ_3 -oxo anion (trigonality indices τ 0.77–0.88).¹⁹ The remaining two zinc ions ($\text{Zn}1$ and $\text{Zn}1\text{A}$) adopt distorted octahedral coordination geometries, being coordinated by six nitrogen atoms from three chelating ligands, and possess the same chirality. Thus, this pentanuclear structure may be considered as a supramolecular triple-strand helicate, in which $[\text{Zn}_3(\mu\text{-O})]^{4+}$ cluster core is wrapped by two terminal, homochiral $[\text{Zn}(\text{H}_2\text{L})_3]^-$ units. However, **1** crystallizes in the centric space group $P2_1/n$ as a racemic mixture of chiral pentanuclear units ($\Delta\Delta$, $\Lambda\Lambda$) showing propeller-shaped supramolecular structures with *M* or *P* helicity (Figure 5).

It is notable that each cluster of **1** involves abundant intramolecular π - π stacking interactions. As shown in Figure 4c, all aromatic rings of H_2L^- possess significant offset face-to-face π - π stacking interactions with closest interplanar and centroid-centroid separations are in 3.05–3.37 and 3.52–4.67 Å, respectively. Besides, there also exists edge-to-face $\text{C}-\text{H}\cdots\pi$ interactions with $\text{H}\cdots$ aromatic ring plane distances ca. 2.77 Å. Such multiple, strong π - π stacking interactions may play an important role in stabilizing the pentanuclear $[(\text{Zn}_3(\mu_3\text{-O})(\text{H}_2\text{L})_6)]^{2+}$ cations.

2 crystallizes in the space group $P\bar{1}$, consisting two pentanuclear units in the asymmetric unit. Each pentanuclear unit of **2** is isostructural with that of **1**. However, some structural differences arise from the different metal ions are also observed. The pentacoordinate $\text{Cd}(\text{II})$ ions show more distorted trigonal-bipyramidal geometries (τ 0.54–0.84) than those of **1**. Besides, the face-to-face π - π stacking interactions (closest interplanar and centroid-centroid separations are in 3.17–3.45 and

(19) The trigonality index τ ($\tau = 0$ denotes ideal square pyramidal; $\tau = 1$ denotes ideal trigonal bipyramidal) was calculated according to the literature. See: Addison, A. W.; Rao, T. N.; Reedijk, J.; van Rijn, J.; Verschoor, G. C. *J. Chem. Soc., Dalton Trans.* **1984**, 1349.

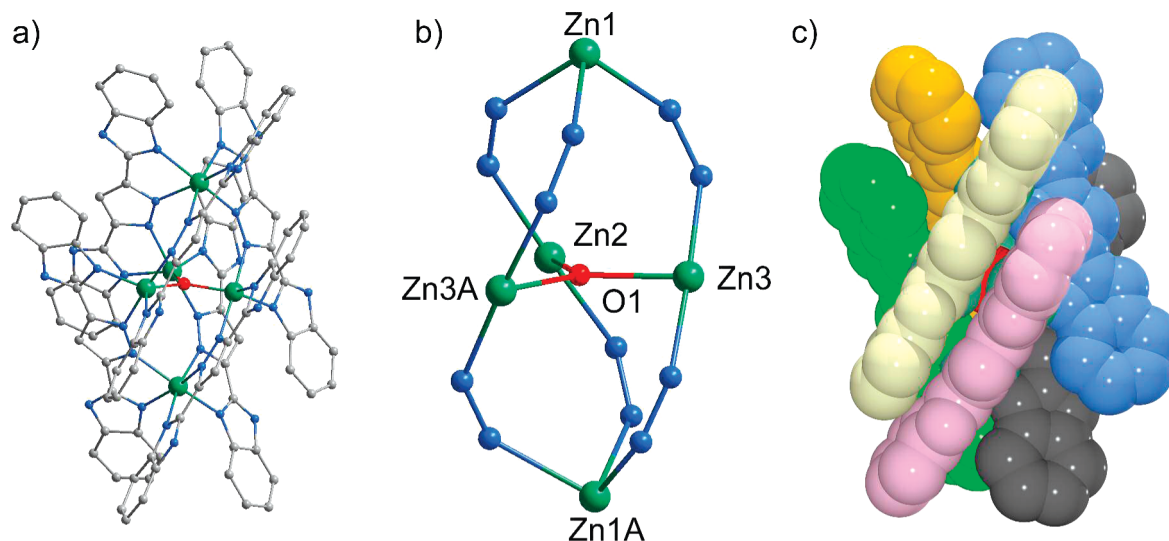


Figure 4. Perspective views of the $\Delta\Delta$ -configurational cation (a), trigonal-bipyramidal core (b), and space-filling drawing (c) of $\Delta\Delta$ -configurational unit of $[\text{Zn}_5(\mu_3\text{-O})(\text{H}_2\text{L})_6]^{2+}$ in **1**. Hydrogen atoms are omitted and each H_2L^- ligand is represented in a different color, while the zinc ions are shown in dark-green and the oxygen atom is in red. Symmetry Codes: (A) $-x + 3/2, -x, y + 1/2$.

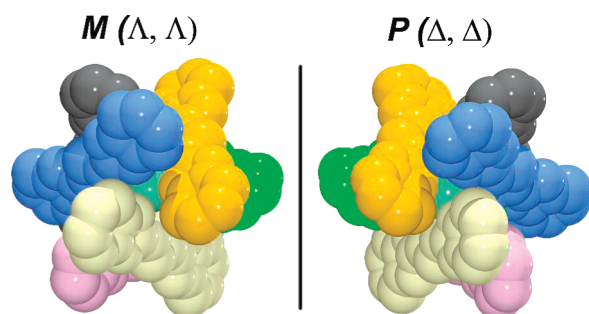


Figure 5. Space-filling representation of the two enantiomers present in **1** viewed down the C_3 axis. For clarity hydrogen atoms are omitted and each H_2L^- ligand is represented in a different color, with zinc ions are represented by dark-green color.

3.98–4.70 Å, respectively) and weaker $\text{C-H}\cdots\pi$ interactions ($\text{H}\cdots\text{aromatic ring plane}$ distances ca. 2.94 Å) demonstrate that the outer shell of **2** is looser than that of **1**. These structural features are consistent with the aforementioned ^1H NMR analyses and the stability differences.

Because of the disorder of the anion and solvent molecules and the quality of the diffraction data, the single-crystal structure of **3** could not be refined properly. However, the preliminary structural solution gives a similar pentanuclear unit as that of **2** (Figure S7 in the Supporting Information).

X-ray crystallographic analysis reveals that **4** has a heptanuclear $\text{Cd}(\text{II})$ structure constructed by six H_2L^- ligands, one $\mu_4\text{-PO}_4^{3-}$ and three $\mu\text{-Br}^-$ ions, which bear a crystallographic 3-fold axis symmetry. As shown in Figure 6a, being similar to the pentanuclear $\text{Zn}(\text{II})/\text{Cd}(\text{II})$ complexes, it also shows a propeller-like structure with three pairs of parallel aligned bis-bidentate H_2L^- ligands arranged around the heptanuclear, turbineate $\text{Cd}(\text{II})$ core (Figure 6b and 6c). However, only one $\text{Cd}(\text{II})$ atom (Cd1) adopts a slightly distorted octahedral geometry by coordination with six nitrogen atoms from three H_2L^- ligands. The whole supramolecular P/M helicity of the cluster can be defined by the Δ/Λ -configuration of this metal atom. The three $\text{Cd}(\text{II})$ atoms (Cd2/Cd2A/Cd2B) in the middle of turbineate core are

crystallographically equivalent; each shows a highly distorted square-pyramidal geometry (trigonality index τ 0.38), being ligated by four nitrogen atoms from two H_2L^- ligands and one oxygen atom of the PO_4^{3-} . The three $\text{Cd}(\text{II})$ atoms (Cd3/Cd3A/Cd3B) at the top of cluster core are also crystallographically equivalent, each adopts a five-coordinate, distorted square-pyramidal geometry constructed by two nitrogen atoms from one H_2L^- , two $\mu\text{-Br}$, and one oxygen from $\mu_4\text{-PO}_4$ (trigonality index τ = 0.35).

There are also extensive intramolecular $\pi\text{-}\pi$ stacking interactions in **4**: offset face-to-face $\pi\text{-}\pi$ stacking with the interplanar and centroid–centroid distances are in the range of 3.40–3.45 and 3.55–3.65 Å, respectively, and edge-to-face $\text{C-H}\cdots\pi$ interactions with $\text{H}\cdots\text{aromatic ring plane}$ distances are 2.80 Å. Although the heptanuclear unit of **4** has three pairs of H_2L^- ligands with $\pi\text{-}\pi$ stacking interaction as those observed in **1–3**, it only possesses one six-coordinate $\text{Cd}(\text{II})$, which makes the whole structure like a cup filled with a PO_4^{3-} anion and capped with a Cd_3Br_3 crown. To the best of our knowledge, no similar heptanuclear complex has been reported so far.

Optical Properties. As **1** and **2** are relatively stable in the solution, the optical properties of **1** and **2** in DMF were investigated by UV–vis and fluorescence spectroscopy. The absorption spectra of **1** and **2** exhibit essentially the same absorption profiles with an intense and low lying (near-UV region) absorption bands with the absorption maxima at 308 nm (Figure S8 in the Supporting Information), which should be ascribed to intraligand $\pi \rightarrow \pi^*$ transition of H_2L^- comparable to that of the free ligand H_3L (Figure S9 in the Supporting Information).

At room temperature, **1** and **2** display bright blue fluorescent emission (Figure 7). Upon excitation at 319 nm, **1** shows a broad emission with the maximum located at 436 nm with the emission lifetime of 10.3 ns (Figure S10 in the Supporting Information), whereas the free H_3L ligand displays a typical ligand-based fluorescent emission as evident by the obvious vibronic structure, small Stokes shift, and short fluorescent lifetime (Figure S11 and S12 in the

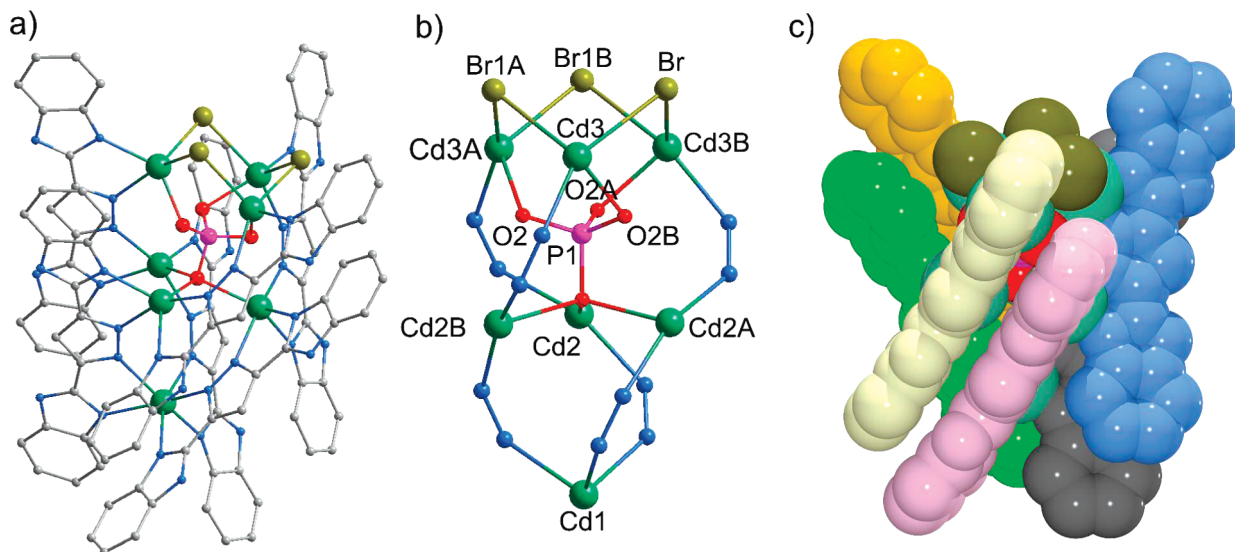


Figure 6. Perspective views of (a) the Δ -configurational cation, (b) the turbinate cluster core, and (c) space-filling drawing of Δ -configurational in $[\text{Cd}_7(\mu_4\text{-PO}_4)(\mu\text{-Br})_3(\text{H}_2\text{L})_6]^{2+}$ cation in **4**. The hydrogen atoms are omitted for clarity and each H_2L^- ligand is represented in a different color; P purple, O red, Cd dark green, Br brown. The symmetry codes are as follows: (A) $-y + 1, z - 1/2, -x + 1/2$; (B) $-z + 1/2, -x + 1, y - 1/2$.

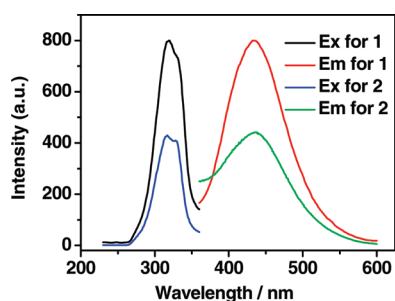


Figure 7. Excitation and emission spectra of **1** and **2** in 1×10^{-6} M DMF solution.

Supporting Information). Because **1** and **2** show large Stokes shifts (ca. 8400 cm^{-1}) and structureless emission profiles, we tentatively assign them to metal-perturbed ligand-centered transitions, probably mixed with some LMCT character.²⁰ The emission character of a freshly prepared DMF solution of **2** is similar to that of **1** with an emission maximum at 434 nm. However, the emission intensity at 434 nm decreases and the intraligand emission increases as the solution stands for 3 days (Figure S13 in the Supporting Information). The change of emission spectrum of **2** is in accordance with its slow decomposition in solution. The emission lifetime of **1** is longer than that of the freshly prepared **2** (2.64 ns, 76.84%, 7.99 ns, 23.16%), which can be ascribed to the tighter structure and stronger intramolecular π - π stacking interactions of **1**.

- (20) (a) Wen, L.-L.; Li, Y. Z.; Dang, D.-B.; Tian, Z.-F.; Ni, Z.-P.; Meng, Q.-J. *J. Solid State Chem.* **2005**, *178*, 3336. (b) Sang, R. L.; Xu, L. *Inorg. Chem.* **2005**, *44*, 3731. (c) Lin, X.-J.; Shen, Z.; Xu, H.-J.; Li, Y.-Z.; Zhang, H.-T.; You, X.-Z. *Inorg. Chem. Commun.* **2004**, *7*, 1167. (d) Zang, S.-Q.; Su, Y.; Li, Y.-Z.; Ni, Z.-P.; Meng, Q.-J. *Inorg. Chem.* **2006**, *45*, 174–180. (e) Zheng, S.-L.; Yang, J.-H.; Yu, X.-L.; Chen, X.-M.; Wong, W.-T. *Inorg. Chem.* **2004**, *43*, 830. (f) Tao, J.; Yin, X.; Wei, Z.-B.; Huang, R.-B.; Zheng, L.-S. *Eur. J. Inorg. Chem.* **2004**, 125. (g) Kutal, C. *Coord. Chem. Rev.* **1990**, *99*, 213. (h) Valeur, B. *Molecular Fluorescence: Principles and Applications*; Wiley-VCH: Weinheim, 2002. (i) Zheng, S.-L.; Zhang, J.-P.; Chen, X.-M.; Huang, Z.-L.; Lin, Z.-Y.; Wong, W.-T. *Chem.-Eur. J.* **2003**, *9*, 3888.

Conclusions

In summary, propeller-like, trigonal-bipyramidal pentanuclear complexes and a turbinate heptanuclear complex are constructed by self-assembly of Zn(II) and Cd(II) ions with a bis-bidentate aromatic *N*-heterocyclic ligand. Unlike other 2-fold symmetric bis-bidentate ligands with a long, flexible spacer that are generally used for the construction of helicates,²¹ the planar H_3L ligand is short and rigid. In the process of self-assembly of these pentanuclear and heptanuclear complexes, aromatic stacking interactions may play an important role in increasing the structural stabilities. ESI-MS studies and ^1H NMR analyses show that the pentanuclear compounds have different solution stabilities depending on the metal ions and counteranions. We have observed the first examples of pentanuclear helicates in solution. The luminescent properties of these clusters are elucidated by their molecular structures and solution behaviors.

Acknowledgment. This work was supported by the “973 Program” (2007CB815302) and Science and Technology Department of Guangdong Province (No. 04205405).

Supporting Information Available: Crystal data (CIF files, additional structural data, and plots), ESI-MS analyses, and ^1H NMR and $\{^1\text{H}-^1\text{H}\}$ COSY NMR spectra for **2**, ^1H NMR spectrum for **3**, photoluminescence data. This material is available free of charge via the Internet at <http://pubs.acs.org>.

IC8007969

- (21) (a) Piguet, C.; Bercardinelli, G.; Bocquet, B.; Schaad, O.; Williams, A. F. *Inorg. Chem.* **1994**, *33*, 4112. (b) Ronson, T. K.; Adams, H.; Riis-Johannessen, T.; Jeffery, J. C.; Ward, M. D. *New J. Chem.* **2006**, *30*, 26. (c) Goetz, S.; Kruger, P. E. *Dalton Trans.* **2006**, 1277. (d) Yeh, R. M.; Raymond, K. N. *Inorg. Chem.* **2006**, *45*, 1130. (e) Ziegler, M.; Davis, A. V.; Johnson, D. W.; Raymond, K. N. *Angew. Chem., Int. Ed.* **2003**, *42*, 665. (f) Mamula, O.; Zelewsky, A. v.; Bercardinelli, G. *Angew. Chem., Int. Ed.* **1998**, *37*, 289.